Supplementary Information

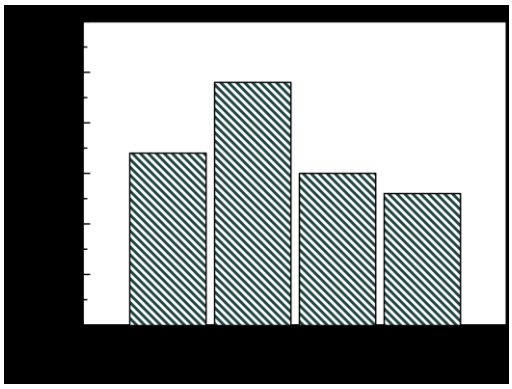

Fig. S1 Absorbance measured at 650 nm showing the normalised ELISA response of the phage particles displaying the four selected binding proteins when exposed to 200 nM of human IL-8 proteins. Binding protein 2 was chosen as the capture protein for the biosensor.

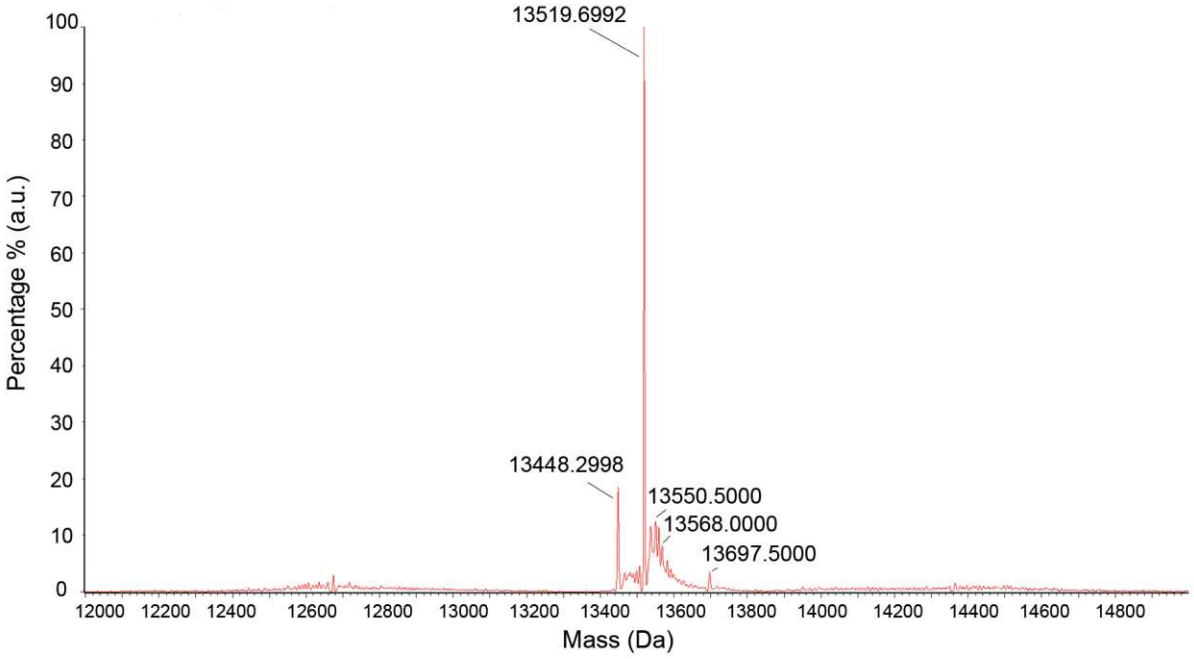

Fig. S2 Mass spectrum of the non-antibody capture protein. The molecular weight of the IL-8 specific binding protein was found to be 13.520 kDa, matching the expected value. The predominant species was confirmed to be lacking alanine with a minor component lacking N-terminal Met. Additional peaks in the spectrum are the results of common modifications associated with cytoplasmically expressed proteins.

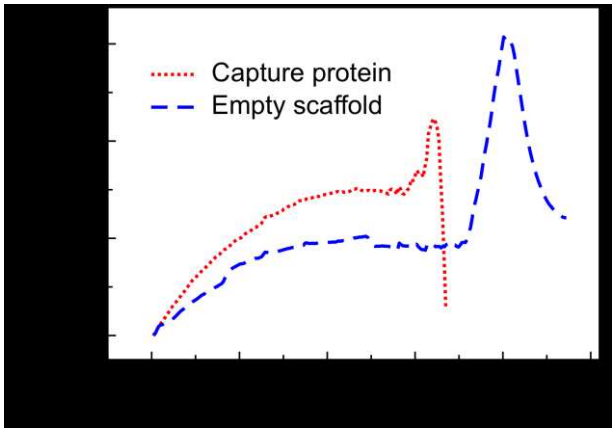

Fig. S3 Heat capacity as a function of temperature showing a melting temperature T_m of 82 ˚C for the non-antibody capture protein, compared to 101 ˚C for the empty scaffold (i.e. the scaffold protein alone without binding loops inserted).

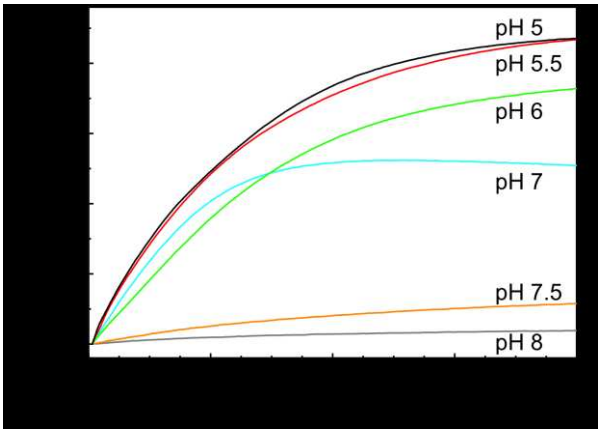

Fig. S4 SPR sensograms recorded to determine optimal coupling conditions for binding proteins as a function of pH onto the monoalkane-thiol-PEG acid monolayer surface on a gold electrode. 10 mM phosphate buffer was used for pH 8–6, and 10 mM acetate buffer was used for pH 5.5–4.5.

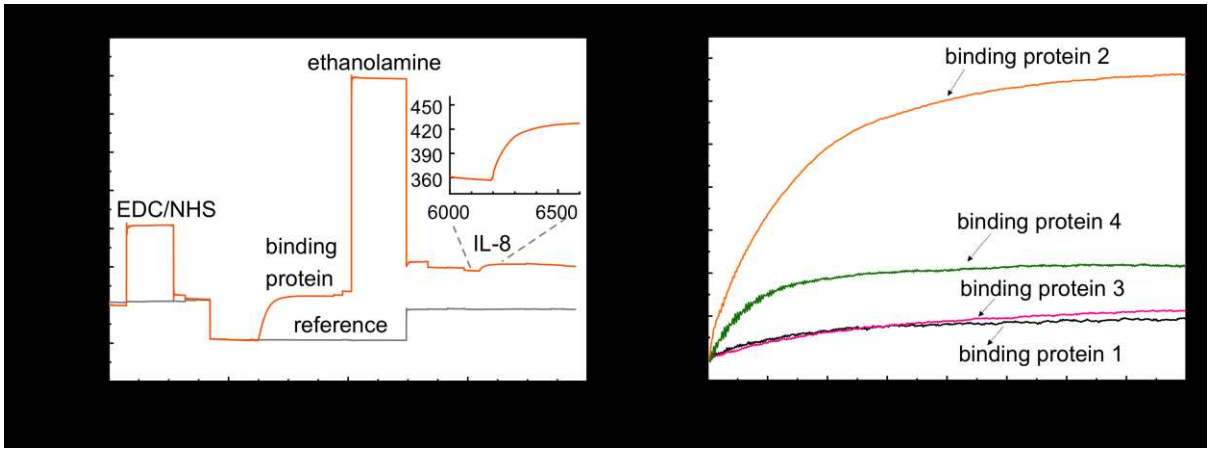

Fig. S5 SPR sensograms showing (a) the immobilisation of the non-antibody binding proteins on the SAM functionalised gold electrode, and the binding of human IL-8 proteins at 1 µg/ml in 100 mM phosphate buffer pH 7, and (b) the binding of IL-8 proteins at 1 µg/ml concentration in 100 mM phosphate buffer pH

7 to sensor surfaces functionalised with four different non-antibody binding proteins selected via phage display. The binding protein showing the highest SPR response (binding protein 2) was chosen as the capture molecule for the subsequent biosensor work.

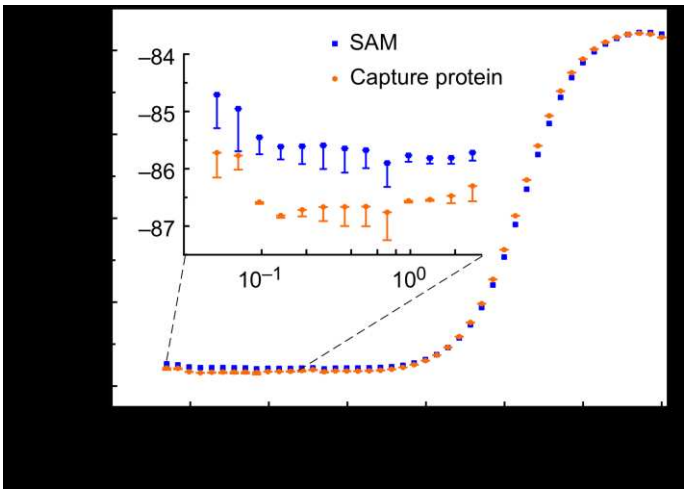

Fig S6: EIS Bode plot showing $\theta(f)$ upon immobilisation of the non-antibody capture proteins on the SAM at a dc offset of 0 mV vs Ag/AgCl. The data shown represent the average of five EIS scans.

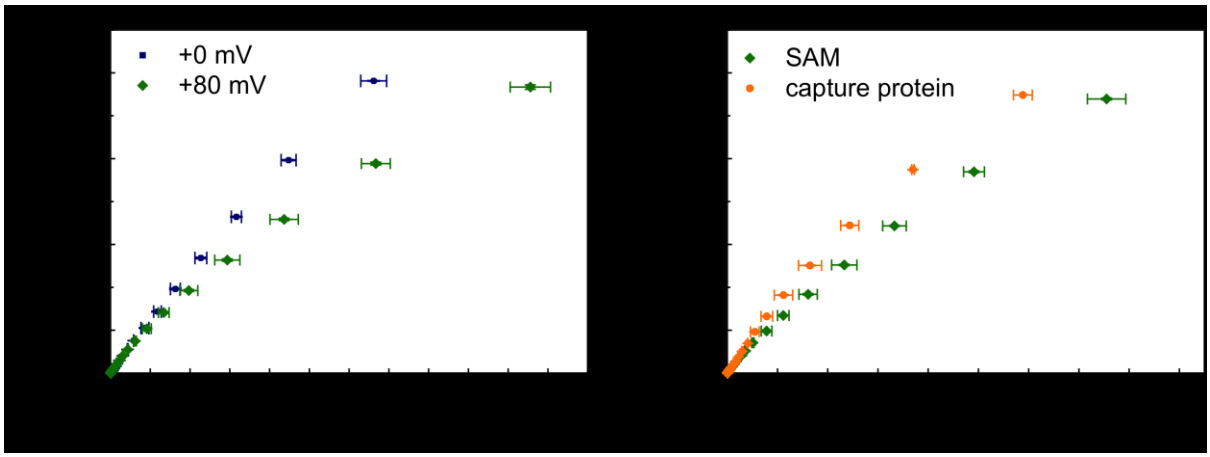

Fig S7: Nyquist plots showing the imaginary versus the real impedance of the sensor after (a) the formation of the monothiol-alkane-PEG acid SAM on the gold electrode at 0 mV and +80 mV dc potential, and (b) the immobilisation of the non-antibody capture molecules on the SAM in comparison to the SAM only at a dc offset potential of +80 mV vs Ag/AgCl. The EIS measurements were conducted in 100 mM phosphate buffer at pH 7 and the data shown represent the average of five EIS scans.

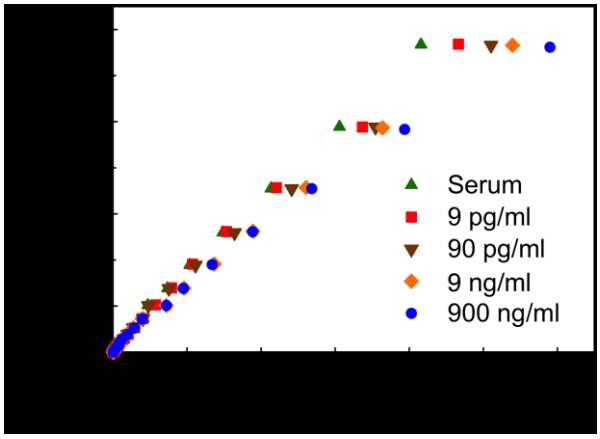

Fig S8: Nyquist plot showing the change in response of the sensor from the baseline response vs IL-8 concentration between 9 fg/ml and 900 ng/ml.

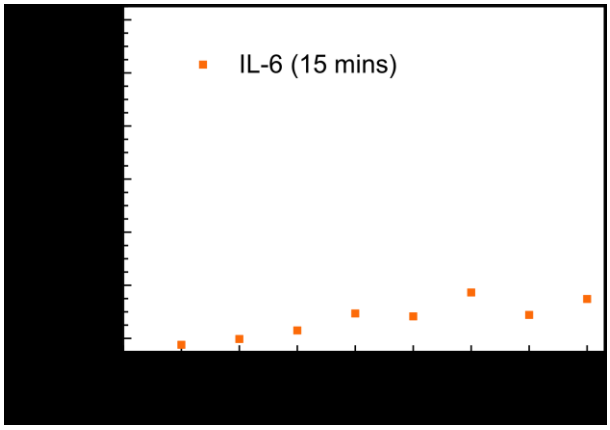

Fig S9: EIS sensogram showing the change in phase from the baseline at 0.1 Hz, $\Delta\theta(f)_{0.1\text{Hz}}$, of the sensor response when exposed to human IL-6 in 100 mM phosphate buffer pH 7 at concentrations between 10 fg/ml and 100 ng/ml. All EIS scans were performed at a dc offset of +100 mV vs Ag/AgCl.